Acknowledgment. This work is supported in part by NIH Grant CA51992 to Frank McCormick of Chiron Corp., who also supplied us with the N-*ras* plasmids; NIH Training Grants GM08313 and GM07598 (RGL); and an NIH postdoctoral fellowship, CA 08872 (C.J.H.). We are grateful to Emil Pai and Ilme Schlichting for access to unpublished atomic coordinates of p21, to Mary Papastavros for technical assistance in the preparation of the protein samples, to Rebecca Meyers for assistance with the GC/MS analysis, and to Steve Branch for helpful discussions about the GC/MS procedures. We also thank George Reed for originally suggesting ESEEM experiments on p21.

Appendix: Comments on Mn^{2+} ESEEM

In the Mn^{2+}·GDP complexes of p21, the $S = {}^5/_2$ multilevel electron spin system is adequately regarded as comprised of noninteracting, resonant two-level systems with constituent levels characterized by the quantum number M_s. The ESEEM response of a nucleus coupled to Mn^{2+} can be described as a sum of the responses associated with each two-level system, weighted by its contribution to the spin–echo. The weights vary with the position of microwave excitation within the EPR powder pattern. The weights are readily calculated in a manner analogous to that which we introduced for the determination of orientational selectivity factors.[14,26,27]

For nuclear spin $I = {}^1/_2$ systems, the two-pulse ESEEM response from each two-level system may be written as:

$$E(\tau) = 1 - (k/4)[2 - 2\cos(2\pi\nu_\kappa\tau) - 2\cos(2\pi\nu_\lambda\tau) + \cos(2\pi(\nu_\kappa - \nu_\lambda)\tau) + \cos(2\pi(\nu_\kappa + \nu_\lambda)\tau)] \quad (1)$$

in which:

$$k = \left[\frac{3\nu_n A_2^0 \cos\theta\,(M_s^\kappa - M_s^\lambda)}{\nu_\kappa\nu_\lambda}\right]^2 \quad (2)$$

and ν_κ or ν_λ are given by:

$$\nu_{\kappa,\lambda} = [(\nu_n + M_s^{\kappa,\lambda}A_0^0 + M_s^{\kappa,\lambda}A_2^0(1 - 3\cos^2\theta))^2 + (3M_s^{\kappa,\lambda}A_2^0 \sin\theta\cos\theta)^2]^{1/2} \quad (3)$$

In eqs 1 - 3, τ is the time between microwave pulses, ν_n is the nuclear Larmor frequency, ν_κ and ν_λ are the nuclear frequencies in the κ and λ electron spin levels, A_0^0 is the isotropic hyperfine coupling constant, A_2^0 is the anisotropic hyperfine coupling constant, and θ is the angle between the external field and the major axis of the hyperfine interaction.

As detailed in previous work,[20] the modulation depth parameter, k, attains its maximum value when, in either the κ or λ spin level, the hyperfine and Zeeman interactions are equal in magnitude and opposed in sign, or "matched". This match occurs within a limited range of nuclear Zeeman frequencies bounded by $|M_s(A_0^0 + 2A_2^0)|$ and $|M_s(A_0^0 - A_2^0)|$. A line-narrowing of the fundamental ESEEM peaks occurs in this same ν_n range. This effect is readily recognized by rewriting expression 3 as:

$$\nu_{\kappa,\lambda} = [(\nu_n + M_s^{\kappa,\lambda}(A_0^0 - A_2^0))^2 + 3M_s^{\kappa,\lambda}A_2^0\cos^2\theta\,(2\nu_n + M_s^{\kappa,\lambda}(2A_0^0 + A_2^0))]^{1/2} \quad (4)$$

from which it is seen that the dispersion caused by the anisotropy of the hyperfine interaction is suppressed, that is, the final term of eq 4 is cancelled, when $\nu_n = |M_s(2A_0^0 + A_2^0)/2|$ and the Zeeman and hyperfine interactions are of opposite sign. The matching of the Zeeman and hyperfine interactions, with attendant amplitude resonance and line-narrowing effects, are primary factors in determining the appearance ESEEM spectra.[19,20] In systems of high electron spin multiplicity, a sequence of matching and line-narrowing situations occurs associated with the succession of allowed values of $|M_s|$.

(26) Gerfen, G. J.; Singel, D. J. *J. Chem. Phys.*, submitted for publication.
(27) Cosgrove, S. A. Applications of Electron Spin Echo Envelope Modulation Spectroscopy to Catalytic Systems. Ph.D. Thesis, Harvard University, 1992.

EXAFS Evidence for a "Cysteine Switch" in the Activation of Prostromelysin

Richard C. Holz,[‡] Scott P. Salowe,[§] Catherine K. Smith,[§,†] Gregory C. Cuca,[§] and Lawrence Que, Jr.*[,‡]

Contribution from the Department of Chemistry, University of Minnesota, Minneapolis, Minnesota 55455, and the Department of Biophysical Chemistry, Merck Research Laboratories, Rahway, New Jersey 07065. *Received April 20, 1992*

Abstract: Zn K-edge EXAFS data of the matrix metalloproteinase (MMP) stromelysin-1 were obtained in both its latent proenzyme and mature active forms. The Fourier-filtered (back-transform 0.7–2.3 Å) χk^3 spectrum of mature stromelysin was satisfactorily simulated with 4 N/O scatterers per Zn at 2.01 Å, while similar fits for prostromelysin were judged unacceptable because of unreasonable Debye–Waller factors or significantly larger residuals of the fits. For prostromelysin, excellent fits were obtained with the introduction of a sulfur scatterer at 2.25 Å. These data provide the first direct evidence for the coordination of zinc by the sole cysteine in the N-terminal domain of prostromelysin and confirm that the cysteine is lost upon activation. These results provide support for a "cysteine switch" structural model for MMP proenzymes that suggests the interaction of the conserved propeptide cysteine with zinc is present in the latent form. Examination of the Zn–S bond length and outer shell carbon contributions suggests that the 2 g-atoms of zinc recently shown to be present in stromelysin (Salowe, S. P., et al. *Biochemistry* **1992**, *31*, 4535–4540) reside in independent zinc sites.

Introduction

Stromelysin-1 is a metalloendoproteinase which is able to degrade a broad range of extracellular components in connective tissue matrices and may be a central agent in the proteolytic destruction of cartilage proteoglycans associated with osteo- and rheumatoid arthritis. Stromelysin is one member of the matrix metalloproteinase (MMP) family of enzymes which are characterized by their high primary sequence similarity, requirement for Ca^{2+} and Zn^{2+}, and secretion as inactive proenzymes.[1] It was recently demonstrated that the N-terminal catalytic domain of stromelysin-1, in fact, contains two zinc sites, with one site clearly

[‡] University of Minnesota.
[§] Merck Research Laboratories.
[†] Present address: Department of Molecular Biophysics & Biochemistry, Yale University, New Haven, CT.

(1) Woessner, J. F. *FASEB J.* **1991**, *5*, 2145–2154.

0002-7863/92/1514-9611$03.00/0 © 1992 American Chemical Society

Table I. Selected Restricted Fits of the First-Coordination-Sphere Fourier-Filtered Zn K-Edge EXAFS Spectra of Stromelysin in Its Latent, Mature, and Zinc-Depleted Forms

		first shell			second shell			
	fit[b]	N/O	r(Å)	σ^2	S/Cl	r(Å)	σ^2	F[a]
[Zn{HB(3-*t*-Bupz)$_3$}Cl]	1	4	2.04	0.001				0.335
	2	1	1.94	−0.004				0.254
		3	2.07	−0.005				
	3	4	2.05	0.004	1	2.19	0.002	0.085
	4	3	2.04	0.001	1	2.21	0.003	0.065
prostromelysin	5	5	2.01	0.005				0.260
	6	4	2.01	0.003				0.269
	7	3	2.05	−0.001				0.238
		1	1.91	−0.003				
	8	4	2.01	0.004	1	2.22	0.010	0.165
	9	3	2.00	0.001	1	2.25	0.005	0.102
	10	3.5	2.00	0.001	0.5	2.25	0.001	0.108
mature stromelysin	11	5	2.01	0.004				0.297
	12	4	2.01	0.003				0.139
	13	3	2.00	0.001	1	2.21	0.207	0.133
	14	3	2.01	0.000				0.122
		1	2.12	0.048				
zinc-depleted stromelysin	15	4	2.01	0.003				0.285
	16	3	2.01	0.001				0.128
	17	2	2.01	−0.001	1	2.30	0.033	0.170
	18	2	2.01	−0.001				0.106
		1	1.95	0.011				

[a] *F*, the goodness of fit, is defined as the rms(dev)/rms(dat), where the function minimized is $R \equiv \{\Sigma k^6(\chi_c - \chi)^2/n\}^{1/2}$.[11] [b] Back-transform window 0.7 to 2.3 Å.

involved in catalysis and inhibitor binding.[2] Although the metal-coordinating amino acids in MMPs are unknown, the histidines present in the strictly conserved sequence HExxHxxGxxH are likely zinc ligands based on the crystal structures of other metalloendoproteinases.[3,4]

The activation of prostromelysin and other MMP proenzymes requires the loss of approximately 80 amino acids from the N-terminus in a complex, multistep process that is not completely understood.[1,5] Their latency has been attributed to the interaction of a cysteine residue in the highly conserved propeptide sequence PRCGVPDV with the active site zinc atom.[6] Replacement of this "cysteine switch" ligand with a water molecule by one of several pathways is believed to create the catalytically competent active site. While indirect evidence from mutagenesis and biochemical studies supports this model,[7,8] there has been no direct demonstration of a Zn–cysteine interaction in a MMP proenzyme. Extended X-ray absorption fine structure (EXAFS) spectroscopy is particularly well suited to clarify this type of structural problem since the sensitivity of EXAFS toward heavy atom scatterers that reside in the inner coordination sphere of metal centers is well documented.[9] Reported herein is the comparison of Zn K-edge EXAFS data of the catalytic domain of human stromelysin-1 in both the latent proenzyme and mature active forms.

Experimental Section

Model Complexes. Several previously reported zinc model complexes which have been crystallographically characterized were synthesized according to published procedures. These included Zn(acac)$_2$·H$_2$O, Zn(Im)$_6$, Zn(OAc)$_2$·2H$_2$O, Zn(Et$_2$dtc)$_2$, and Zn(Me$_2$dtc)$_2$.[10-15] Additionally, the potential proenzyme model [Zn{HB(3-*t*-Bupz)$_3$}Cl] (**1**), was synthesized.[16]

Preparation of Protein Samples. The catalytic domain of prostromelysin containing the N-terminal 255 residues was purified as previously described.[17] The corresponding mature form was prepared by heat treatment and gel filtration. Zinc-depleted mature enzyme was prepared by dialysis versus *o*-phenanthroline.[2] All three samples contained protein between 2.4 and 3.0 mM in 50 mM Tris·HCl pH 7.5 with 10 mM CaCl$_2$ and 20% v/v glycerol to prevent ice crystal formation. The prostromelysin sample also contained 1 mol % inhibitor U24278[18] to prevent autolytic activation. The metal content of the pro- and mature samples was 1.9 and 1.8 mol equiv of Zn, respectively, while the depleted sample contained only 0.9 equiv.

EXAFS Data Collection and Analysis. X-ray absorption spectra (XAS) were collected between 9.5 and 10.5 keV at station C-2 of the Cornell High Energy Synchrotron Source (CHESS). The monochromator was calibrated using the 9660.0-eV K-edge of Zn foil. The XAS data of the protein samples were obtained at 100 K, while data for the models were collected at ambient temperature. A large solid-angle Lytle fluorescence detector was used with a Cu filter and Soller slits. The treatment of the raw EXAFS data to yield χ and the refinements reported on χk^3 data minimized with the function $R \equiv \{\sum k^6(\chi_c - \chi)^2/n\}^{1/2}$ (where $k = [8\pi^2 m_e(E - 9660\text{ eV} + \Delta E)/h^2]^{1/2}$ and $\chi_c = \sum_{\text{shells}}\{nA[f(k)k^{-1}r^{-2}e^{-2\sigma^2k^2}\sin(2kr + \alpha(k))]\}$ has been previously discussed in detail.[19] In this analysis procedure, previously reported crystal structures of several zinc complexes (Zn(acac)$_2$·H$_2$O, Zn(Im)$_6$Cl$_2$·4H$_2$O, Zn(OAc)$_2$·2H$_2$O, Zn(Et$_2$dtc)$_2$, and Zn(Me$_2$dtc)$_2$) were used to determine the amplitude reduction factor (A) and the shell-specific edge shift (ΔE) for

(2) Salowe, S. P.; Marcy, A. I.; Cuca, G. C.; Smith, C. K.; Kopka, I. E.; Hagmann, W. K.; Hermes, J. D. *Biochemistry* **1992**, *31*, 4535–4540.
(3) Vallee, B. L.; Auld, D. S. *Biochemistry* **1990**, *29*, 5647–5659.
(4) Bode, W.; Gomis-Rüth, F. X.; Huber, R.; Zwilling, R.; Stöcker, W. *Nature* **1992**, *358*, 164–167.
(5) Nagase, H.; Enghild, J. J.; Suzuki, K.; Salvesen, G. *Biochemistry* **1990**, *29*, 5783–5789.
(6) Van Wart, H. E.; Birkedal-Hansen, H. *Proc. Natl. Acad. Sci. U.S.A.* **1990**, *87*, 5578–5582.
(7) Windsor, L. J.; Birkedal-Hansen, H.; Birkedal-Hansen, B.; Engler, J. A. *Biochemistry* **1991**, *30*, 641–647.
(8) Park, A. J.; Matrisian, L. M.; Kells, A. F.; Pearson, R.; Yuan, Z. *J. Biol. Chem.* **1991**, *266*, 1584–1590.
(9) (a) Scott, R. A. *Methods Enzymol.* **1985**, *117*, 414–459. (b) Teo, B.-K. In *EXAFS Spectroscopy, Techniques and Applications*; Teo, B.-K., Joy, D. C., Eds.; Plenum: New York, 1981; pp 13–58.
(10) Abbreviations used: acac = acetylacetonate; Im = imidazole; OAc = acetate; Et$_2$dtc = diethyldithiocarbamate; Me$_2$dtc = dimethyldithiocarbamate; HB(3-*t*-Bupz)$_3$ = hydrotris(3-*tert*-butyl-1-pyrazolyl)borate.
(11) Mongomery, H.; Lingafelter, E. C. *Acta Cryst.* **1963**, *16*, 748–752.
(12) Sandmark, C.; Bränen, C.-I. *Acta Chem. Scand.* **1967**, *21*, 993–999.
(13) van Niekerk, J. N.; Schoening, F. R. L.; Talbot, J. H. *Acta Cryst.* **1953**, *6*, 720–723.
(14) Bonamico, M.; Mazzone, G.; Vaciago, A.; Zambonelli, L. *Acta Cryst.* **1965**, *19*, 898–909.
(15) Klug, H. P. *Acta Cryst.* **1966**, *21*, 536–546.
(16) Gorrell, I. B.; Looney, A.; Parkin, G. *J. Chem. Soc., Chem. Commun.* **1990**, 220–222.
(17) Marcy, A. I.; Eiberger, L. L.; Harrison, R.; Chan, H. K.; Hutchinson, N. I.; Hagmann, W. K.; Cameron, P. M.; Boulton, D. A.; Hermes, J. D. *Biochemistry* **1991**, *30*, 6476–6483.
(18) Caputo, C. B.; Wolanin, D. J.; Roberts, R. A.; Sygowski, L. A.; Patton, S. P.; Caccese, R. G.; Shaw, A.; DiPasquale, G. *Biochem. Pharmacol.* **1987**, *36*, 995–1002.
(19) (a) Scarrow, R. C.; Maroney, M. J.; Palmer, S. M.; Que, L., Jr.; Roe, A. L.; Salowe, S. P.; Stubbe, J. *J. Am. Chem. Soc.* **1987**, *109*, 7857–7864. (b) True, A. E.; Orville, A. M.; Pearce, L. L.; Lipscomb, J. D.; Que, L., Jr. *Biochemistry* **1990**, *29*, 10847–10854. (c) True, A. E.; Scarrow, R. C.; Randall, C. R.; Holz, R. C.; Que, L., Jr. *J. Am. Chem. Soc.*, submitted for publication.

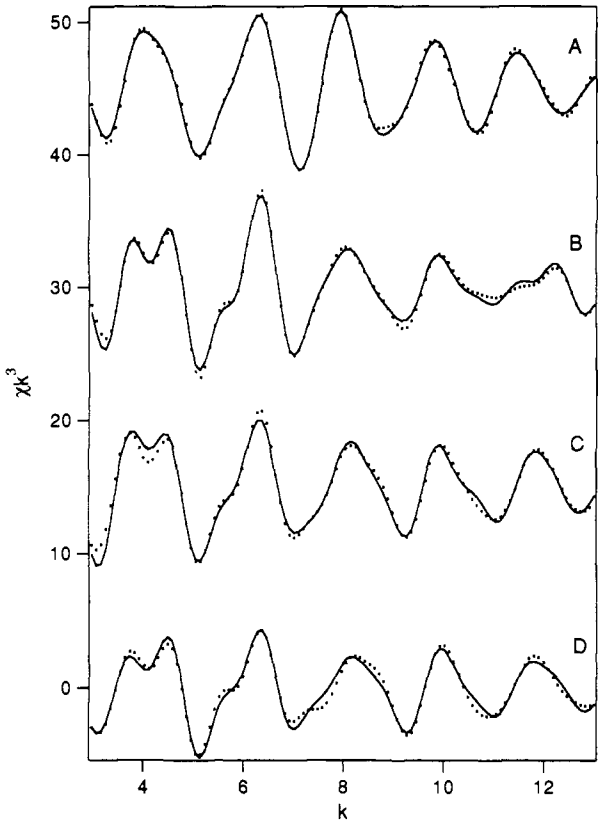

Figure 1. Smoothed and Fourier-filtered (back-transform 0.7–4.0 Å) χk^3 data (●) with four and five shell restricted fits (—) for **1** (A), prostromelysin (B), mature stromelysin (C), and zinc-depleted stromelysin (D). All stromelysin data were obtained in the fluorescence mode on frozen solutions at ca. 100 K. The simulations correspond to fits 19, 22, 24, and 25, respectively (Table II).

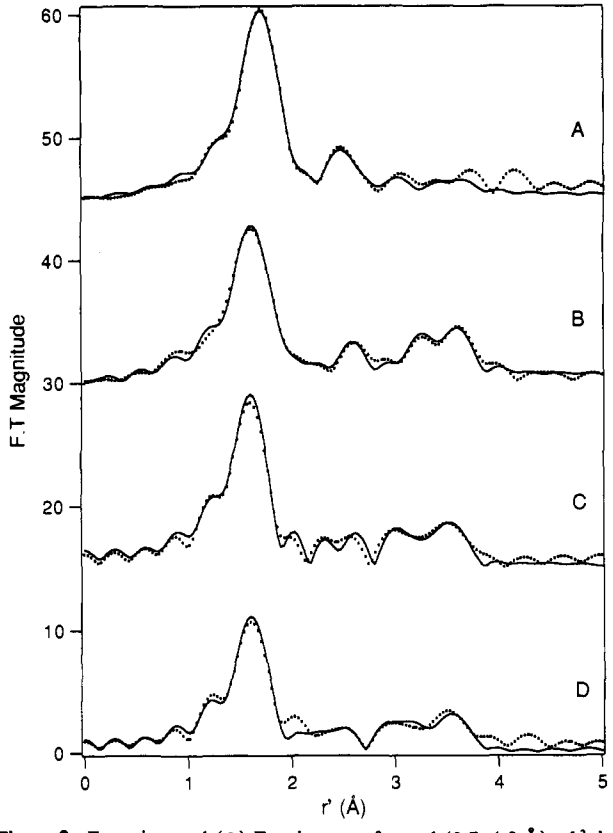

Figure 2. Experimental (●) Fourier-transformed (0.7–4.0 Å) χk^3 data for **1** (A), prostromelysin (B), mature stromelysin (C), and zinc-depleted stromelysin (D). The solid lines represent five shell restricted fits (Table II fits 19, 22, 24, and 25, respectively).

Zn–O/N, Zn–S, and Zn–C interactions. This leaves two parameters per shell, the distance (r) and the Debye–Waller factor (σ^2) or the number of atoms (n), to be refined instead of the four parameters refined using BFBT ("best fit based on theory").[20]

Results and Discussion

Zn K-edge EXAFS data were obtained for [Zn{HB(3-*t*-Bupz)$_3$}Cl][16] (**1**), prostromelysin, stromelysin, and a zinc-depleted derivative preparation (Figure 1). These data were analyzed as previously described based on several structurally characterized zinc model compounds with coordinated N/O or S atoms.[10-15] The Fourier-filtered EXAFS spectrum of **1**, a potential model for the putative metal site of the proenzyme with three Zn–N bonds and one Zn–Cl bond, was simulated by 3 N/O scatterers at 2.04 Å and 1 Cl scatterer at 2.21 Å (fit 4, Table I). These bond lengths are in good agreement with the crystallographically determined bond lengths of a closely related compound.[16] Attempts to simulate the data with only N/O scatterers in single or multiple shells, or with less than 1 Cl scatterer did not reproduce the data well based on their Debye–Waller factors and the residuals of the fits (fits 1–3, Table I). The Debye–Waller factor of a particular shell provides a measure of the vibrational disorder and distribution of bond lengths for that shell. Based on the model data, a σ^2 value of ~0.005 Å adequately models the vibrational disorder of that shell.

The Fourier-filtered EXAFS data for pro- and mature stromelysin are shown in Figure 1. An excellent single shell fit of the Fourier-filtered (back-transform 0.7–2.3 Å) χk^3 spectrum of the mature enzyme was obtained with 4 N/O scatterers per Zn at 2.01 Å (fit 12, Table I). Since stromelysin has recently been shown to contain 2 g-atoms of zinc in the N-terminal catalytic domain,[2] the EXAFS data reveal an average of both zinc environments. The addition of a second shell of N/O donor atoms did not significantly improve the fit or did not adequately reproduce the data based on the Debye–Waller factors (fit 14, Table I). Inclusion of 0.5 or 1 S scatterer at ca. 2.25 Å provided unacceptable fits in all cases (fit 13, Table I). EXAFS data for a zinc-depleted sample that contains zinc only in the noncatalytic site of the protein was also obtained and is quite similar to that of mature stromelysin. An excellent fit was obtained with 3 N/O scatterers at 2.01 Å (fit 16, Table I). The inclusion of more N/O scatterers or multiple shells provided no significant improvement in the fits or gave significantly poorer fits (fit 18, Table I). Similar to the mature enzyme, the inclusion of a S scatterer provided a fit with an unacceptable Debye–Waller factor (fit 17, Table I). These data indicate that neither sulfur nor chloride ion from the added $CaCl_2$ is present in the inner-coordination sphere of the zinc ions in either the mature or zinc-depleted enzymes.

Excellent first-sphere fits of the Fourier-filtered (back-transform 0.7–2.3 Å) χk^3 spectrum of prostromelysin were obtained with a principal shell of 3 or 3.5 N/O scatterers per Zn at 2.00 Å and 1 or 0.5 S scatterers per Zn at 2.25 Å (fits 9 and 10, Table I). Attempts to model the Fourier-filtered first-sphere EXAFS data of prostromelysin without a heavy atom scatterer such as sulfur resulted in fits with significantly larger residuals (fits 5 and 6, Table I). Furthermore, the inclusion of a second shell of N/O scatterers did not result in a significant improvement in the residual and afforded unreasonable Debye–Waller factors (fit 7, Table I). Because cysteine-75 is the only amino acid in the proenzyme which can supply a thiolate ligand, these data provide direct evidence for the coordination of this propeptide residue to zinc in prostromelysin and confirm that the sulfur scatterer is lost upon activation.

Since comparable fits for prostromelysin were obtained with 0.5 or 1 S scatterer per Zn, the cysteine ligand may be terminally bound to only one of the two zinc atoms (giving a sulfur coordination number of 0.5 per Zn) or may bridge the two zinc ions in a dinuclear site (affording a sulfur coordination number of 1

(20) Teo, B.-K.; Antonio, M. R.; Averill, B. A. *J. Am. Chem. Soc.* **1983**, *105*, 3751–3762.

Table II. Selected Restricted Fits of Fourier-Filtered Zn K-Edge EXAFS Spectra of Stromelysin Samples

		first shell			second shell			third shell			
	fit[b]	O/N	r(Å)	σ^2	S/Cl	r(Å)	σ^2	C	r(Å)	σ^2	F[a]
[Zn{HB(3-*t*-Bupz)$_3$}Cl]	19	3	2.04	0.001	1	2.21	0.002	7.2	2.92	0.006	0.082
								3.9	3.31	0.005	
								3.9	3.98	0.008	
prostromelysin	20	3	2.00	0.001	1	2.25	0.004	4.2	2.99	0.002	0.115
								7.2	3.64	0.007	
								10.3	3.99	0.005	
	21	3	2.03	0.002	1	2.25	0.006	3.4	3.00	0.001	0.150
								1[c]	3.70	0.008	
								14.6	3.99	0.005	
	22	3.5	2.00	0.001	0.5	2.25	0.001	4.3	3.00	0.002	0.117
								7.4	3.64	0.007	
								10.2	3.99	0.005	
mature stromelysin	23	4	2.01	0.002				6.5	3.19	0.019	0.182
								1[c]	3.28	0.007	
								10.4	3.99	0.006	
	24	4	2.01	0.002				4.8	3.06	0.008	0.176
								4.2	3.35	0.003	
								10.4	3.99	0.006	
zinc-depleted stromelysin	25	3	2.01	0.001				2.9	2.82	0.008	0.175
								3.8	3.37	0.004	
								10.5	3.98	0.007	

[a] *F*, the goodness of fit, is defined as the rms(dev)/rms(dat), where the function minimized is $R \equiv [\Sigma k^6(\chi_c - \chi)^2/n]^{1/2}$.[11] [b] Back-transform window 0.7 to 4.0 Å. [c] A single zinc atom was used in these fits.

per Zn). While coordination numbers derived from EXAFS have significant uncertainties, the bond distances are accurate to within 0.02 Å.[9] Thus ambiguities related to the thiolate coordination mode may be resolved by considering the structural implications of the Zn–S bond length. Examination of structurally characterized Zn(II)–SR complexes indicate that bridging thiolates typically have Zn–S bonds greater than 2.35 Å, while terminal thiolates in complexes with nitrogen-rich environments have Zn–S bonds less than 2.30 Å.[21] Furthermore, EXAFS analyses of zinc enzymes with one or two terminal cysteines have Zn–S bond lengths less than 2.33 Å.[22-24] Since the observed Zn–S bond distance in prostromelysin is 2.25 Å, a terminal thiolate and hence two independent Zn(II) sites are favored.

Analysis of the Fourier-filtered (back-transform 0.7–4.0 Å) χk^3 spectra of the three stromelysin samples showed the presence of low Z scatterers between 2.8 and 4 Å (Figure 2). Carbon shells at these distances are typically observed due to multiple scattering effects of the imidazole ring atoms of histidine residues and thus indicate histidine coordination to the zinc center; a similar set of low Z scatterers is also found for **1** which arises from the pyrazole ring atoms (Table II). Furthermore, the second shell data of each of the stromelysin samples are visually very similar to those of several protein mononuclear zinc sites that contain histidine residues.[23,24]

Alternatively, the second shell features of both mature and prostromelysin at 3.28 and 3.70 Å, respectively, could also be modeled by a Zn scatterer. However, the residuals of the fits and/or the Debye–Waller factors were significantly better for the low Z scatterer alternatives, suggesting the presence of two independent zinc sites (compare fits 21 and 22 for prostromelysin and fits 23 and 24 for mature stromelysin, Table II). Furthermore, the Zn–S–Zn angle of 110.6° for prostromelysin derived from fit 21 is inconsistent with the structures of synthetic zinc thiolate complexes.[21] For comparison, the largest Zn–S–Zn angle found in synthetic complexes is 100° for the tetranuclear zinc complex of *N*,*N*′-dimethyl-*N*,*N*′-bis(β-mercaptoethyl)ethylenediamine,[21b] which reflects the tendency of sulfur to adopt bond angles of near 90° in metal complexes. Such an angle would require a Zn–Zn distance of 3.45 Å in prostromelysin, given a Zn–S bond length of 2.25 Å. Therefore, a bridging cysteine is unlikely and the second shell features are more consistent with carbon scatterers, suggesting two independent zinc sites for prostromelysin.

In conclusion, detailed analysis of the first-sphere Fourier-filtered EXAFS data of pro- and mature stromelysin has provided the first direct evidence of a cysteine ligand coordinated to zinc in prostromelysin, consistent with a "cysteine switch" structural model[6] for the MMP family of enzymes. These data also suggest that the 2 equiv of zinc in the enzyme resides in independent zinc sites.

Acknowledgment. This work was supported by a grant from the National Science Foundation (Grant No. DMB-9104669, L. Q.). R.C.H. is grateful for an NIH postdoctoral fellowship (GM-13919). We wish to thank the operators at the Cornell High Energy Synchrotron Source (CHESS) which is supported by the National Science Foundation (DMR-8412465). We thank Ms. Catherine Chiou for providing compound **1**, Dr. William Hagmann for supplying U24278, and Mr. Clayton R. Randall and Drs. Anne E. True and Timothy E. Elgren for help in data collection.

(21) See, for example: (a) Watson, A. D.; Rao, C. P.; Dorfman, J. R.; Holm, R. H. *Inorg. Chem.* **1985**, *24*, 2820–2826. (b) Hu, W. J.; Barton, D.; Lippard, S. J. *J. Am. Chem. Soc.* **1973**, *95*, 1170–1173. (c) Cohen, B.; Mastropaolo, D.; Potenza, J. A.; Schugar, H. J. *Acta Cryst.* **1978**, *34B*, 2859–2860. (d) Bell, P.; Sheldrick, W. S. *Z. Naturforsch.* **1984**, *39B*, 1732–1737. (e) Corwin, D. T., Jr.; Koch, S. A. *Inorg. Chem.* **1988**, *27*, 493–496.

(22) Diakun, G. P.; Fairall, L.; Klug, A. *Nature* **1986**, *324*, 698–699.

(23) Feiters, M. C.; Jeffery, J. *Biochemistry* **1989**, *28*, 7257–7262.

(24) Dent, A. J.; Beyersmann, D.; Block, C.; Hasnain, S. S. *Biochemistry* **1990**, *28*, 7822–7828.